Photocycloaddition of Phenanthrene with Acetylacetonatoboron Difluoride: Exciplex Reactions

Yuan L. Chow,* Susan P. Wu, and Xinxin Ouyang

Department of Chemistry, Simon Fraser University, Burnaby, British Columbia, Canada V5A 1S6

Received September 1, 1993•

In dioxane or ether singlet excited phenanthrene (PN) reacts with acetylacetonatoboron difluoride ($AABF_2$) irreversibly to form a fluorescent exciplex with a well-defined isosbestic point in the low range of $[AABF_2] \leq 0.03$ M. This exciplex is shown to be the precursor to the observed product of *cis*-9-acetyl-9,10-dihydro-10-(2-oxopropyl)phenanthrene by quantitative quenching analysis of the product and fluorescence. In contrast, the excitation of $AABF_2$ in the presence of PN gives neither exciplex emission nor any products. The exciplex was studied on the basis of its static and time-resolved fluorescence properties to give the dipole moment of 11.2 D and its reaction pattern. The exciplex undergoes self-quenching by $AABF_2$, and the quantum yield carries dependency on the square of its concentrations that would impose a nonlinear relation in the double reciprocal plot of $1/\Phi$ *vs* $1/[AABF_2]$. The plot started to curve upward at $[AABF_2]$ as low as 0.02 M owing to simultaneous complication from the competing and unproductive absorption by $AABF_2$, particularly at a high concentration range. Experimentally, the isosbestic point is unfocused at $[AABF_2] \geq 0.025$ M to indicate a small effect of self-quenching. In acetonitrile singlet excited PN preferentially undergoes electron transfer to give the phenanthrene cation radical without causing the cycloaddition.

Introduction

Phenanthrene (PN), on excitation, undergoes [2 + 2] photocycloadditions with many types of olefins to give cyclobutane derivatives[1] (e.g., 1 in Scheme 1); these photoreactions have served as models among others to bridge the concept of exciplexes in photophysics and photochemistry.[1-10] These developments also coincide with photoinduced electron transfer,[1] which constitutes one of the important driving forces for exciplex formations. Among a number of demonstrations that exciplexes are viable and natural precursors,[1-4] the work using singlet excited PN is most direct and elegant by correlating the rate of the product formation and exciplex decay under complex kinetic conditions.[2,5] These pioneer works led to a general acceptance and ubiquitous assumption of exciplexes in bimolecular photoreactions.

Acetylacetonatoboron difluoride ($AABF_2$) reacted from its singlet excited state with benzene to give a high yield of the [2 + 2] photocycloadduct[11] which underwent secondary reactions. In contrast, the present photoaddition observed in a mixture of PN and $AABF_2$ shows that excited-state PN is actually the species initiating the reaction. Evidence established in this work demonstrates that it is an exciplex which is the immediate precursor of cycloaddition. As the present case appears to be uncomplicated from triplet and energy transfer reactions,[1,2,5,6] we have studied the dynamics of the exciplex formation and reactions.

Scheme 1

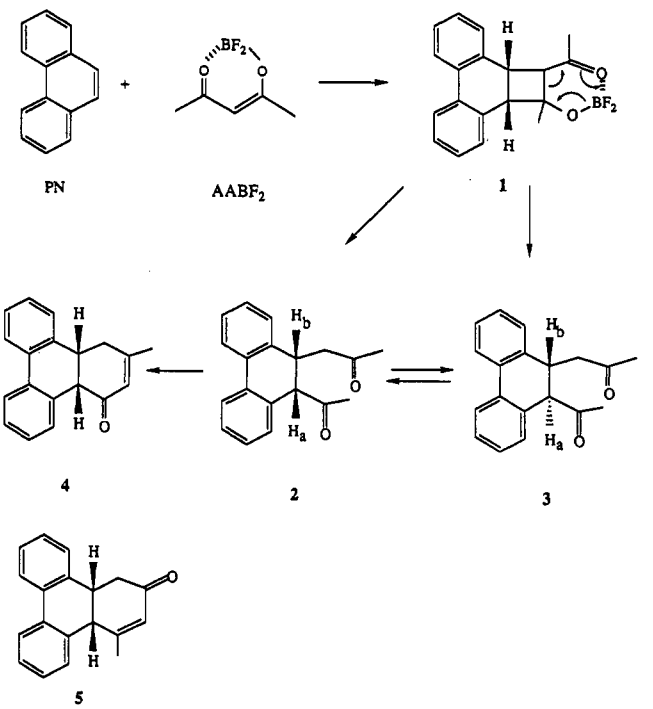

Results

Photocycloaddition. PN and $AABF_2$ were photolyzed in ether or dioxane to give an excellent yield of *cis*-1,5-

• Abstract published in *Advance ACS Abstracts*, January 1, 1994.

(1) (a) Caldwell, R. A.; Creed, D. *Acc. Chem. Res.* **1980**, *13*, 45. (b) Mattes, S. L.; Farid, S. *Acc. Chem. Res.* **1982**, *15*, 80. (c) Lewis, F. D. *Acc. Chem. Res.* **1979**, *12*, 152. (d) McCullough, J. J. *Chem. Rev.* **1987**, *87*, 811.

(2) (a) Caldwell, R. A.; Smith, *J. Am. Chem. Soc.* **1974**, 2994. (b) Caldwell, R. A.; Ghali, N. I.; Chien, C. K.; DeMarco, D.; Smith, L. *J. Am. Chem. Soc.* **1978**, *100*, 2857. (c) Caldwell, R. A. *J. Am. Chem. Soc.* **1973**, *95*, 1690. (d) Caldwell, R. A.; Creed, D.; De Marco, D. C.; Melton, L. A.; Ohta, H.; Wine, P. H. *J. Am. Chem. Soc.* **1980**, *102*, 2369.

(3) (a) Creed, D.; Caldwell, R. A. *J. Am. Chem. Soc.* **1974**, *96*, 7369. (b) Caldwell, R. A.; Creed, D. *J. Am. Chem. Soc.* **1979**, *101*, 6960.

(4) Caldwell, R. A.; Mizuno, K.; Hansen, P. E.; Vo, L. P.; Frentrup, M.; Ho, C. D. *J. Am. Chem. Soc.* **1981**, *103*, 7263.

(5) (a) Creed, D.; Caldwell, R. A.; Ulrich, M. M. *J. Am. Chem. Soc.* **1978**, *100*, 5831. (b) Caldwell, R. A.; Maw, T. S. *J. Photochem.* **1979**, *11*, 165.

(6) (a) Farid, S.; Doty, J. C.; Williams, J. C. R. *J. Chem. Soc., Chem. Commun.* **1972**, 711. (b) Farid, S.; Hartman, S. E.; Doty, J. C.; Williams, J. C. R. *J. Am. Chem. Soc.* **1975**, *97*, 3687.

(7) Mizuno, K.; Pac, C.; Sakurai, H. *J. Am. Chem. Soc.* **1974**, *96*, 2993.

(8) McCullough, J. J.; MacInnis, W. K.; Lock, C. J. L.; Faggiani, R. *J. Am. Chem. Soc.* **1982**, *104*, 4644.

(9) Yang, N. C.; Masnovi, J.; Chiang, W. L.; Wang, T. Y.; Shou, H. S.; Yang, D. D. H. *Tetrahedron* **1981**, *37*, 3285 and other papers in this series.

(10) DeSchryver, F. C. et al. *Pure Appl. Chem.* **1977**, *49*, 237.

(11) (a) Chow, Y. L.; Ouyang, X. X. *Can. J. Chem.* **1991** *69*, 423. (b) Chow, Y. L.; Cheng, X. E. *J. Chem. Soc., Chem. Commun.* **1990**, 1043.

0022-3263/94/1959-0421$04.50/0

diketone **2** and a trace amount of the corresponding *trans*-isomer **3** as in Scheme 1; as the irradiation used a Rayonet RPR 3500 Å light source, mainly PN was excited. For solution in [PN] = 0.02 M and [$AABF_2$] = 0.02 M, the quantum yield of **2** was 0.10 in dioxane and 0.015 in ether under nitrogen, this was reduced to 45% and 0% under air and pure oxygen, respectively. The formation of *trans*-**3** was insignificant, never exceeded 2–3% after 4–6 h irradiation, and was most likely formed secondarily from the isomerization of the *cis*-isomer. In acetonitrile no photoreaction occurred under comparable conditions. Also, in the presence of high concentrations of a triplet sensitizer, such as benzophenone or xanthone (0.2 M), similar irradiation caused no cycloaddition or other photoreactions. Since benzophenone was the primary absorber of light in the system and, also, its photoreduction products were not obtained, triplet energy transfer must have occurred to generate triplet excited PN. Both isomers *cis*-**2** and *trans*-**3** were photostable in dioxane and acetonitrile either in the presence or absence of PN under comparable irradiation conditions.

Isomers *cis*-**2** and *trans*-**3** shared similar ^{13}C NMR, IR, and MS data suggesting that they are stereoisomers. Both ^1H NMR spectra exhibited one doublet (H_a) and one ddd (H_b) for the four-spin system with J_{ab} = 4.6 for **2** and 1.3 Hz for **3**; on the basis of the coupling constants *cis* and *trans* configurations were assigned, respectively, in analogy to the reported J values[12] of some *cis–trans* pairs of 9,10-saturated phenanthrenes. In addition, both isomers showed a very strong IR absorption at 1708–1713 cm^{-1} and two ^{13}C NMR signals each in the 206–209 ppm region. In ether **2** was slowly isomerized to **3**; the yield was only 5–6% in 10 h when stirred in heterogeneous phases with 0.1 N aqueous H_2SO_4. In either 0.2 N $NaOCH_3$–CH_3OH or 0.2 N H_2SO_4–CH_3OH at room temperature, *cis*-**2** underwent aldol condensation to give enone **4** and a trace amount of an isomer which was assumed to be **5**, both of which showed a similar MS pattern. Interestingly, in these treatments the percentage of **3** remained practically unchanged while the percentage of *cis*-**2** was rapidly reduced. Further, the treatment of *trans*-**3** under similar basic conditions did not cause noticeable isomerization to *cis*-**2** but generated a trace amount of the cyclized product. The major enone showed spectral data consistent with either **4** or **5** with a methine proton coupling constant J = 5.0 Hz, i.e., a *cis*-ring fusion. Structure **4** was favored because of (i) a small but finite coupling (J = 0.5 Hz) between the CH_3 and CH_2 groups and (ii) one aromatic proton at a relatively high chemical shift (7.05 ppm) arising from anisotropy of the nearby carbonyl group.

The quantum yield of *cis*-**2** under nitrogen remained constant within experimental errors on variation of [PN] but varied in the range of [$AABF_2$] 0.006–0.040 M at conversions <9%. The plot of Φ^{-1} vs $[AABF_2]^{-1}$ gave a reasonable linear correlation in the low concentration region; but the experimental points started to curve upward at [$AABF_2$] > 0.025 M (Figure 1) in dioxane (and also in ether). The linear portion could be extrapolated to the limit to give K_{sv}^{γ} (= intercept/slope) 460 ± 160 M^{-1} in dioxane and 150 ± 35 M^{-1} in ether according to eq 1 where

$$1/\Phi = 1/\beta + 1/(\beta K_{sv}^{\gamma}[A]) \quad (1)$$

(12) Lewis, F. D.; DeVoe, R. J. *J. Org. Chem.* **1982**, *47*, 889.

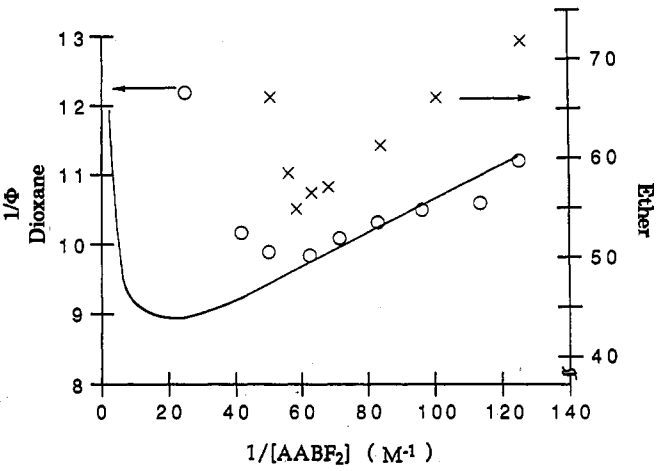

Figure 1. Plot of $1/\Phi$ *vs* $1/[AABF_2]$. The points are experimentally determined, and the solid line is that computed from eq 10 (see Experimental Section) and the rate constants given in Table 3.

Table 1. Stern–Volmer Constant of the Interaction of Singlet Excited PN and Its Exciplex with $AABF_2$[a] in Dioxane

	K_{sv}^{p} (370 nm)[a]	K_{sv}^{x} (480 nm)[b]	K_{sv}^{γ} (Φ)[c]
$AABF_2$	280 ± 5 120 ± 4[d]		(460 ● 160)[g]
1,3-pentadiene	0.41 ± 0.05[e]	2.4 ± 0.2[f]	1.6 ± 0.1[h]
anisole	(<0.2)[e]	10.1 ± 0.3[f] 6.8 ± 0.2[d,f]	10.2 ± 1.0[h] 6.9 ± 0.6[d,h]

[a] Determined from the intensity attenuation at 370 nm with [PN] ≅ 10^{-4} M [$AABF_2$] < 0.024 M. [b] Determined from intensity monitors at 480 and 370 nm according to eq 3. [c] Determined from the quantum yield monitor. [d] These data were obtained under air, while others were obtained under an inert atmosphere. [e] [PN] ≅ 10^{-4} M. [f] [PN] = (40–5) × 10^{-4} M, [$AABF_2$] = 0.08–0.01 M. [g] [PN] = 0.02 M by eq 1; this is an approximate figure. [h] [PN] = 0.02 M, [$AABF_2$] = 0.01–0.015 M, by eq 2.

both K_{sv}^{γ} and β have the usual meaning[13] and will be discussed later. Such double reciprocal plots generally involve large error margins, as will be shown later; in the present case this calculation is only an approximation. In the presence of a quencher (Q), such as 1,3-pentadiene or anisole, the quantum yield of **2** was systematically reduced; through Stern–Volmer plots (eq 2) the quenching was analyzed to give K_{sv}^{γ} values that are listed in Table 1: note that K_{sv}^{γ} here is related to a quencher at constant [$AABF_2$].

$$\Phi^{\circ}/\Phi \text{ or } I^{\circ}/I = 1 + K_{sv}^{\gamma}(\text{or } K_{sv}^{p})[Q] \quad (2)$$

Fluorescence Quenching Studies. PN exhibited strong fluorescence peaks in ether or dioxane in the region of 350–430 nm and, also, phosphorescence peaks at 460, 495, 535, and 585 nm at 77 K. $AABF_2$, on the contrary, showed no emission at all in many solvents; the previously reported fluorescence[14] at [$AABF_2$] > 0.05 M was shown to arise from an impurity which could be eliminated by rigorous recrystallization. PN fluorescence was systematically reduced in the presence of $AABF_2$ (Figure 2). The interaction in the low range of [$AABF_2$] < 0.025 M was analyzed to give Stern–Volmer constant K_{sv}^{p} 120 M^{-1} (air)

(13) (a) Turro, N. J. *Modern Molecular Photochemistry*; The Benjamin/Cummings: Menlo Park, CA, 1978; Chapter 8. (b) Murov, S. L. *Handbook of Photochemistry*; Marcel Dekker: New York, 1973.
(14) Karasev, V. E.; Korotkikh, O. A. *Russ. J. Inorg. Chem.* (*Engl. Transl.*) **1986**, *31*, 493.

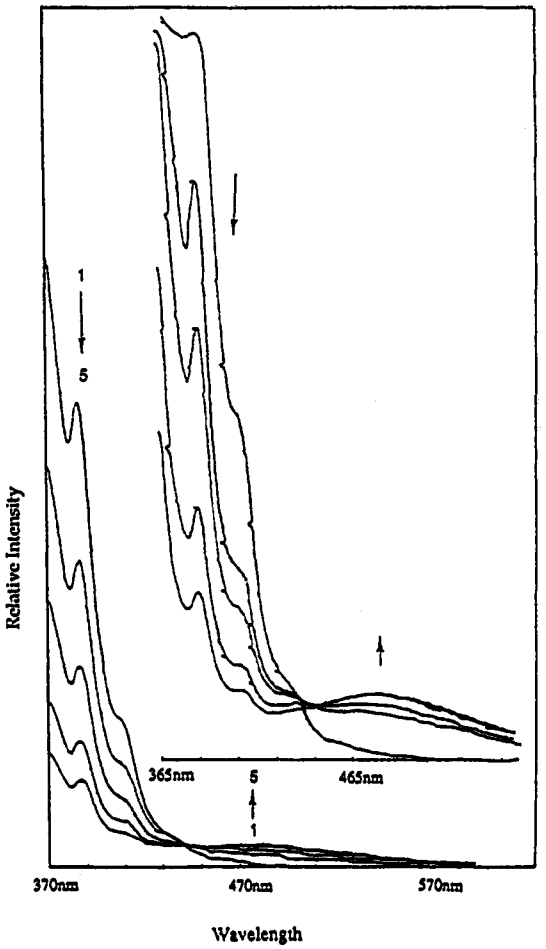

Figure 2. Quenching of PN(5×10^{-4} M) fluorescence intensities by $AABF_2$ (0.002–0.016 M) in dioxane under argon with λ_{ex} = 350 nm. Inset: similar quenching at higher $AABF_2$ concentrations (0.0064–0.052 M) under air.

and 280 M (argon) in dioxane according to the standard eq 2; $K_{sv}^{p} = k_{pq}\tau^{\circ}$ where τ° is the lifetime of singlet excited *PN which interacts with $AABF_2$ with the rate constant of k_{pq} as shown in Scheme 2. The interaction with $AABF_2$ also generated a new broad peak at ca. 480 nm with an isosbestic point at 440 nm in dioxane and 430 nm in ether. Above [$AABF_2$] = 0.035 M, the isosbestic point started to lose its precision, and also, the intensity of exciplex emission ceased to increase regardless of further quenching of PN fluorescence. Indeed, the exciplex intensity began to be reduced at [$AABF_2$] > 0.1 M. In a frozen solution of 2-propanol–ether, neither fluorescence nor phosphorescence of PN was affected by $AABF_2$ up to 0.25 M. This observation ruled out the long-range Coulombic mechanism for the above interaction, which must therefore, occur by physical collisions. For quenching experiments, PN absorption peak at 350 nm was excited in order to avoid $AABF_2$. Also, absorption spectra of PN were not substantially changed in the presence of $AABF_2$ up to 0.2 M, indicating that a ground-state CT complex was not formed. For a series of solutions containing [PN] = 0.0005 or 0.005 M and increasing [$AABF_2$] (0.0005–0.02M) it was excited at 310 nm where both substrates absorbed; the absorption by $AABF_2$ caused drastic decreases in PN fluorescence without causing exciplex emission (see Experimental Section). The same solutions, when excited at 350 nm for PN, displayed the quenching and formation of exciplex fluorescence, such as that shown in Figure 2.

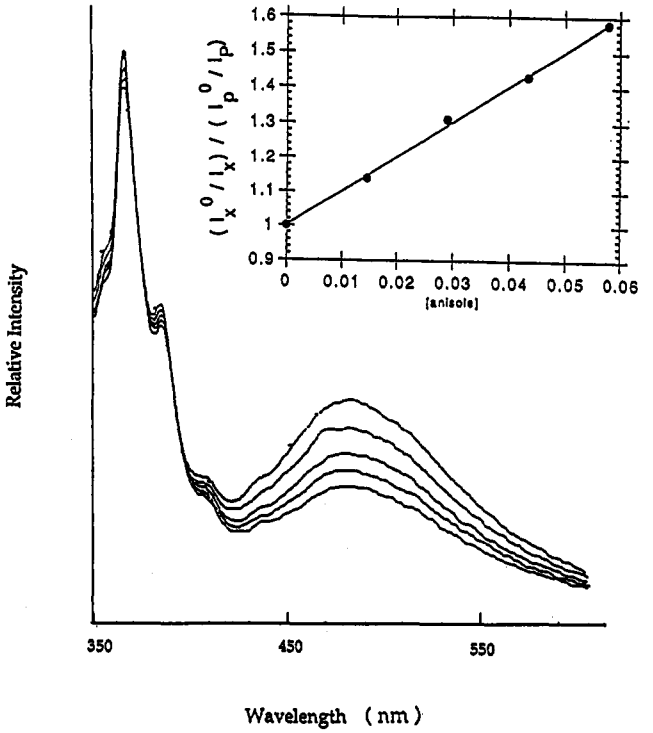

Figure 3. Quenching of fluorescence intensities by anisole (0.015–0.058 M) in dioxane under argon with [PN] = 4.1×10^{-3} M, [$AABF_2$] = 0.10 M, λ_{ex} = 350 nm.

The electronic property of the exciplex was determined by peak shifts of fluorescence maxima caused by solvent polarity. In order to circumvent the requirement to deal with the specific solute–solvent interactions, the observed solvatochromic shifts (ν_{max} in cm^{-1}) were correlated with those of a reference having analogous chemical types.[15] The exciplex of dibenzomethanatoboron difluoride with *p*-xylene has a dipole moment of 10.5 D and was chosen as the reference;[16] wavenumbers (ν_{max}) of maxima in a series of solvents were plotted against each other as in Figure 4. Assuming solvent cavities were the same for the both systems, the dipole moment of the exciplex PN–$AABF_2$ could be calculated from the slope to be 11.2 D (see Experimental Section).

Fluorescence quenching of PN in dioxane and ether was first studied in the absence or presence of a low concentration of [$AABF_2$] < 0.01 M where the exciplex emission was nil or weak; PN fluorescence intensity at 370 nm (I_p) was quenched feebly by 2,5-dimethyl-2,4-hexadiene (K_{sv}^{p} = 4.9 M^{-1}), by 1,3-pentadiene ($K_{sv}^{p} \cong 0.41$ M^{-1}), and anisole ($K_{sv}^{p} < 0.2$ M^{-1}); the Stern–Volmer constants were estimated by eq 2. At higher concentrations of $AABF_2$ (0.01–0.10 M), exciplex fluorescence intensities at 480 nm (I_x) were preferentially quenched over PN fluorescence (I_p) by 1,3-pentadiene and anisole (Figure 3). Exciplex quenching was analyzed by eq 3 derived previously by

$$(I_x^{\circ}/I_x)/(I_p^{\circ}/I_p) = 1 + K_{sv}^{x}[Q] = 1 + k_{xc}\tau_x[Q] \quad (3)$$

$$\tau_x = (\sum k_{x1} + k_{xa} + k_{xr} + k_{xq}[A])^{-1} \quad (4)$$

Caldwell's group[2d] where k_{xc} is the quenching rate constant

(15) Lakowicz, J. R. *Principles of Fluorescence Spectroscopy*; Plenum: New York, 1983; p 194.
(16) Johansson, C. I. Unpublished resutls, Simon Fraser University, 1991.

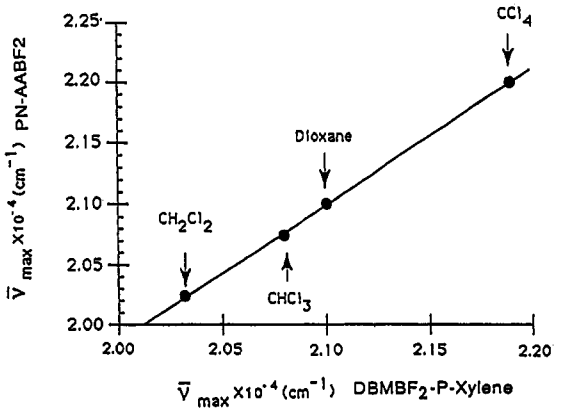

Figure 4. Plot of fluorescence maxima (ν_{max}) of the PN–$AABF_2$ exciplex against those of $DBMBF_2$–*p*-xylene exciplex in CCl_4, dioxane, chloroform, and methylene chloride.

Scheme 2

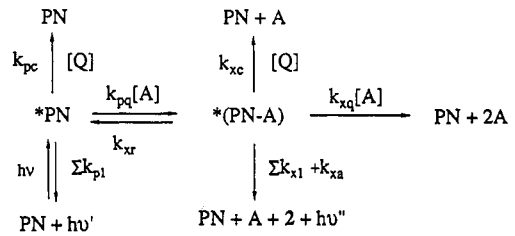

by these quenchers of the exciplex which has the lifetime of τ_x as defined in eq 4 according to Scheme 2 (see below). The Stern–Volmer constants (K^x_{sv}) are listed in Table 1; it was clear these K^x_{sv} values agreed closely with K^y_{sv} values obtained from the quenching of the quantum yields of cycloadduct **2**.

Fluorescence Decay Kinetics and Flash Photolysis. The reactivity of the exciplex was further probed using time-resolved fluorescence decay trace on the basis of the mechanism proposed from the steady-state experiments as in Scheme 2. It is assumed that the exciplexes react to give **2** (k_{xa}) and are quenched by $AABF_2$ (k_{xq}) as suggested by the pattern in Figure 2. The terms $\sum k_{p1}$ and $\sum k_{x1}$ represent the sum of all unimolecular reactions for *PN and the exciplex, respectively, and involve the rate constants of fluorescence decays (k_{pf}, k_{xf}). Using single photon counting techniques, the acquisition of the fluorescence decay data followed the well-established method[17,18] to give decay rates collected in Table 2. The treatment of these decay rates followed the standard method,[17] and the same procedure was used in a similar case;[18] the details were described in the Experimental Section. The lifetime of singlet excited PN was determined in dioxane solution which gives nice single exponential decay traces with lifetimes of 26 (air) and 54 ($\tau°$, argon) ns. The solution containing $AABF_2$ was excited at 350 nm in order to avoid irradiation of this substrate; this generated Raman emission which interfered with the *PN fluorescence peak; only the exciplex decay trace at 470 nm was analyzed as biexponential kinetics to give $\tau_1(=\lambda_1^{-1})$, the residual lifetimes of singlet PN, and $\tau_2(=\lambda_2^{-1})$, the exciplex decay lifetimes (see Table 2). The former were

(17) (a) Ware, W. R. *Pure Appl. Chem.* **1975**, *41*, 635. (b) Birks, J. B. *Prog. React. Kinet.* **1970**, *5*, 188. (c) Lewis, F. D.; Bassani, D. M. *J. Photochem. Photobiol. A: Chem.* **1992**, *66*, 43.

(18) Chow, Y. L.; Johansson, C. I. *J. Photochem. Photobiol. A: Chem.* **1993**, *74*, 171.

(19) Chow, Y. L.; Cheng, X. E. *Can. J. Chem.* **1991**, *69*, 1575.

Table 2. Kinetic Parameters[a] of Singlet Excited PN and the Exciplex with $AABF_2$

$[AABF_2]$ (M)	$\lambda_1 \times 10^{-7}$ s^{-1} (τ_1 in ns)[b]			$\lambda_2 \times 10^{-7}$ s^{-1} (τ_2 in ns)[b]
0.00	1.86 ± 0.02	(53.8)[c]		
0.01	8.4	(11.86)	5.7	(17.44)
0.02	12.5	(7.97)	5.8	(17.15)
0.03	18.4	(5.42)	5.5	(18.32)
0.04	23.1	(4.33)	5.5	(17.27)
0.05	28.6	(3.50)	5.8	(17.22)
0.08	50.2	(1.99)	5.8	(17.34)
0.12	67.2	(1.49)	6.2	(16.17)
0.12[d]			6.1	(16.28)
0.25[d]			7.5	(13.29)
0.30[d]			8.1	(12.34)

[a] [PN] = 5×10^{-5} M in dioxane under argon with λ_{ex} 350 nm. [b] From eqs 6 and 7; $\tau = \lambda^{-1}$. [c] This corresponds to $\tau°$ and τ_1 = 26 ns under air. [d] A separate series of experiments.

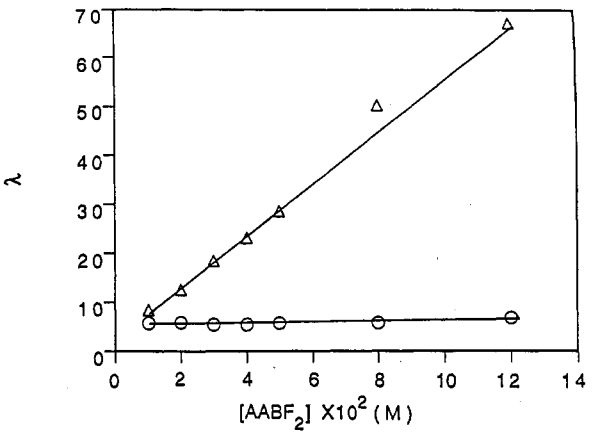

Figure 5. λ_1 or λ_2 *vs* $[AABF_2]$.

Table 3. Interaction of *PN + $AABF_2$ in Dioxane; Rate Constants from Fluorescence Intensity Measurements

$\sum k_{p1}$	$(1.87 \pm 0.02) \times 10^7$ s^{-1}
k_{pq}	$(5.51 \pm 0.11) \times 10^9$ M^{-1} s^{-1}
	5.2×10^9 M^{-1} s^{-1} [a]
	4.6×10^9 M^{-1} s^{-1} [b]
$\sum k_{x1} + k_{xa}$[c]	$(5.7 \pm 0.1) \times 10^7$ s^{-1}
k_{xq}	$(7.2 \pm 0.4) \times 10^7$ M^{-1} s^{-1}
k_{xr}[c]	($<10^6$ s^{-1})
k'_{xc}[d]	5.7×10^8 M^{-1} s^{-1}
k''_{xc}[d]	1.3×10^8 M^{-1} s^{-1}

[a] Calculated from K^p_{sv} obtained in the static quenching experiment under argon. [b] Calculated from K^p_{sv} obtained in the static quenching experiment under air and the reduced lifetime of 26 ns (Table II). [c] Since k_{xr} is insignificant, it is omitted. [d] The rate constants of the exciplex quenching by anisole (k'_{xc}) and 1,3-pentadiene (k''_{xc}) calculated from K^x_{sv} in static quenching experiments in Table I and τ_x = 19 ns.

plotted against $[AABF_2]$ to give $k_{pq} = 5.51 \times 10^9$ M^{-1} s^{-1}, while the latter apparently varied very little up to $[AABF_2]$ = 0.08 M and afforded the exciplex lifetime ($\tau_x°$) of 17 ns (or $\sum k_{x1} + k_{xa} + k_{xr} = 5.7 \times 10^7$ s^{-1}, see Figure 5) at the intercept. The lack of variations in the latter exciplex lifetimes is most likely related to the complex dynamics of exciplex self-quenching and will be elaborated in relation to k_{xq} values. Using the lifetimes determined here, the rate constant of the interaction of *PN with $AABF_2$ (k_{pq}) can be determined from the static fluorescence quenching; in argon $K^p_{sv}/\tau° = (280/54$ ns) $= 5.2 \times 10^9$ M^{-1} s^{-1} and under air ($120/26$ ns $= 4.6 \times 10^9$ M^{-1} s^{-1} (Table 3); these data are very close to k_{pq} obtained above.

Observed decay rates in Table 2 were used to plot $\lambda_1 + \lambda_2$ (Figure 6) or $\lambda_1\lambda_2$ (Figure 7) against $AABF_2$ concen-

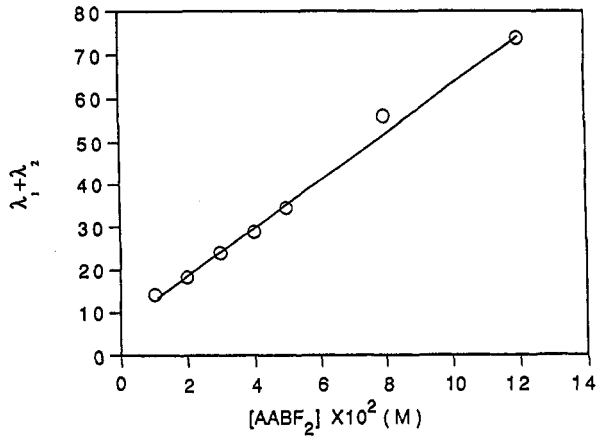

Figure 6. $\lambda_1 + \lambda_2$ *vs* [$AABF_2$].

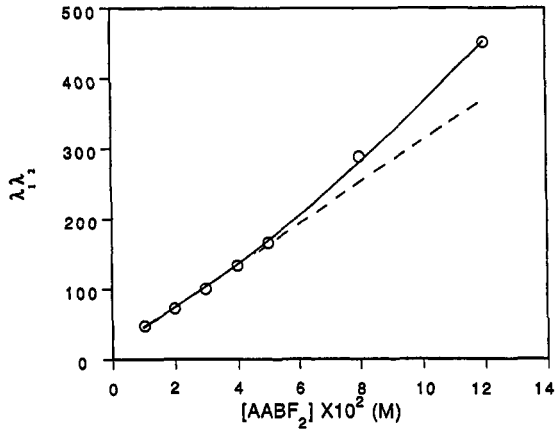

Figure 7. $\lambda_1\lambda_2$ *vs* [$AABF_2$].

trations according to eqs 8 or 9, respectively (see Experimental Section). Figure 7 shows a plot with slight upward curvature indicating small contributions from the quadratic term in eq 9; that is, k_{xq} does exist but is not likely to be big with respect to k_{pq}. The plot in Figure 6 afforded a slope of (5.57 ± 0.22) × 10^9 M^{-1} s^{-1} and intercept of (7.46 ± 0.79) × 10^7 s^{-1}. Appropriate subtractions from these figures showed that calculated k_{xr} (<10^6 s^{-1}) and k_{xq} (6.8 × 10^7 M^{-1} s^{-1}) were part of the experimental errors and only "order-of-magnitude" approximate figures. As the exciplex formation is practically irreversible because of insignificant k_{xr}, k_{xq} could be evaluated independently from the plot of λ_2 against [$AABF_2$], according to $\lambda_2 = \sum k_{x1} + k_{xa} + k_{xq}$[A], at concentrations higher than 0.1 M where virtually all singlet excited PN had been converted to exciplex. Using the last three values of λ_2 in Table 2 the plot gave a slope of 7.6 × 10^7 M^{-1} s^{-1}. The average of two k_{xq} values, 7.2 × 10^7 M^{-1} s^{-1}, is listed in Table 3.

Since the benzophenone-sensitized photoreaction of PN and $AABF_2$ failed, it must be concluded that triplet excited PN does not initiate photoreaction with $AABF_2$; the failure shows an interesting contrast to the triplet excited photoreaction of PN with maleate and fumarates,[2,6] concurrent with the singlet-state reaction. To confirm the lack of triplet reaction, the present photocycloaddition was also investigated with laser-pulsed flash photolysis at 355-nm excitation (YAG laser) using apparatus available in the University of Victoria. In dioxane under argon, PN was excited to show, either in the presence or absence of [$AABF_2$] = 10^{-4}–10^{-2}, a strong transient absorption with the peak at 480 nm which decayed with lifetimes of 20–22 μs. As this long-lived transient was reduced to zero under the air in <3 μs, this absorption was assigned as the T–T absorption of triplet excited PN. The invariance of the lifetimes indicated the lack of triplet state reactions. In acetonitrile, PN was photoexcited in the presence of $AABF_2$ (10^{-3}–10^{-2} M) to give two overlapped transient absorptions at 420 and 480 nm (and also complementary broad absorptions in 700–800 nm) with the lifetimes of 1.6 and 1.2 ms, respectively. As the latter peak intensity was rapidly reduced under the air within 0.5 ms, it was assigned to triplet excited state PN. The remaining signal showed that the absorptions at 400, 430, and 700–800 nm, though not well resolved, were very similar to reported PN cation radical ($PN^{\bullet+}$) absorptions in acetonitrile.[20] In acetonitrile the excitation of PN gave the T–T absorption at 480 nm with the lifetime of 8 μs in analogy to that reported.[20] It was concluded that PN underwent photoinduced electron transfer from both its singlet and triplet states to generate $PN^{\bullet+}$.

Discussion

The photocycloaddition of PN with $AABF_2$ is a clean reaction to give cycloadduct **1** as the primary product which undergoes rearrangement–hydrolysis to afford the final *cis*-1,5-diketone **2**. In the process, a small amount of HF is formed and acts as a catalysis to isomerase **2** to *trans*-**3**. The result described above reveals that singlet excited PN initiates the reaction with $AABF_2$ to give highly stereoselective *cis*-addition through an exciplex without complication from triplet-state pathways such as those observed in similar photoadditions with fumarates and maleates.[2,5] The simplicity of this reaction pattern provides an uncomplicated case for its mechanistic studies that have revealed unambiguously that the exciplex is the precursor of **2** and liable to be quenched by $AABF_2$. Both phenomena have been observed in other photocycloadditions involving phenanthrene derivatives.[2d,3] The treatment of **2** and **3** with an acid or base reveals interesting carbanion reaction patterns. Firstly, *cis*-**2** requires a much lower activation energy to preferentially cyclize to **4** than that to isomerize to **3**. Secondly, *trans*-**3** resists isomerization and cyclization under these mild conditions; the latter cyclization must require the highest activation energy among others. These phenomena must be related to conformational stability of carbanions and warrant a study in the future.

The interaction of singlet excited PN with $AABF_2$ must occur by physical collisions as required by the exciplex formation and is supported by the lack of long-range Coulombic quenching. The exciplex must have substantial CT character as shown by the dipole moment of 11.2 D. While electron transfer must have occurred to generate $PN^{\bullet+}$–$AABF_2^{\bullet-}$, high CT character does not have to mean a favorable factor for the cycloadduct formation,[4,11b] but it may serve to bring the reactants together in specific orientation to generate the observed high degree of *cis*-stereoselectivity. The failure to obtain the photocycloaddition in acetonitrile coupled with the occurrence of $PN^{\bullet+}$ by flash photolysis in the same solvent eloquently demonstrate this point. It is obvious that highly dipolar acetonitrile facilitates early electron transfer from the encounter complex stage at a distance ≥ 10 Å. Such fully

(20) (a) Selwyn, J. C.; Scaiano, J. C. *Can. J. Chem.* **1981**, *59*, 663. (b) Jones, G., II; Schwartz, W.; Malba, V. *J. Phys. Chem.* **1982**, *86*, 2286.

developed ion radical pairs separated by solvent fail to form contact pairs and may collapse by reverse electron transfer to the ground state. While an exact value could not be obtained, the fluorescence decay kinetics demonstrate that the exciplex is formed irreversibly in dioxane, i.e., $k_{xr} \ll \sum k_{x1} + k_{xa}$. The conclusion is confirmed by the close agreement of k_{pq} determined from static and time-resolved quenching experiments[17] as shown in Table 3.

That the exciplex is the direct precursor to the cycloadduct **2** is proven by the good agreement of the quenching constants (K^{y}_{sv}) of the product **2** formation with those of the exciplex fluorescence (K^{x}_{sv}) by 1,5-pentadiene and anisole (Table 1). The distinct disagreement with the quenching constant (K^{p}_{sv}) of *PN fluorescence clearly indicates that singlet excited PN, though it initiates the reaction, is only distantly related to the formation of **2**. The unequivocal proof of the exciplex formation provides a rationale for the clean *cis*-stereoselectivity in the primary step of the cycloaddition. In this respect, the failure of the excitation of $AABF_2$ to pump the photocycloaddition becomes an interesting question. In theory, singlet excited $AABF_2$ ($E_s \cong 90$ kcal/mol at 320 nm) can transfer the excitation energy to PN ($E_s = 83$ kcal/mol);[13] in the process it may, or may not, form an exciplex. Among all possible reasons, the observed lack of energy transfer is most easily explained by a short lifetime (for instance, less than 100 ps) of singlet excited $AABF_2$ which cannot be intercepted without a high concentration of PN. Alternatively, even if an exciplex is formed, it could be different from that shown in Scheme 1; i.e., the exciplex does not fluoresce and possess the necessary configuration to allow energy migration to occur. As *$AABF_2$ shows no fluorescence under all types of conditions, its short lifetime appears to be supported.

While time-resolved fluorimetry is a useful technique to resolve a complex reaction pattern to afford individual rate constants for fast excited-state reactions, in the present case, calculated k_{xq} and k_{xr} are either about the same or even smaller than experimental errors and, therefore, no more than approximate values. Fortunately, the kinetic investigation on the exciplex dynamics is rendered relatively straightforward in the present case by the irreversible exciplex formation. The self-quenching of the exciplex by $AABF_2$ is clearly shown by the shifting of the isosbestic point at $[AABF_2] > 0.025$ M and more directly by decreases in exciplex fluorescence intensities (Figure 2) and decay rates (Table 2) at higher concentrations. The best experimental figure of $k_{xq} = 7.2 \times 10^7$ s^{-1} obtained from time-resolved fluorimetry appears to be rather low to explain that the shifting of the isosbestic point in Figure 2 can start to show at as low as $[AABF_2]$ 0.02–0.03 M. The low figure does indicate that the contributions of self-quenching ($k_{xq}[A]$) up to $[AABF_2] = 0.08$ M is less than 10% of the decay rates of exciplex, λ_2, the small changes of which are beyond the machine capability to differentiate; this is shown by the invariance of the λ_2 plot in Figure 5. The presence of the self quenching step (k_{xq}) poses considerable complexity on the kinetic dissolution of rate processes in eqs 1 and 3; for example, the lifetime of exciplex is dependent on $AABF_2$ concentrations as shown in eq 4. The quenching rate constants k_{xc} are calculated with $\tau_1 = 1/\sum k_{x1} = 19$ ns on the basis of the invariance at $[AABF_2] < 0.08$ M in Figure 5. It must be added that K^{y}_{sv} obtained from the quantum yield monitor in eq 1 also contains the effect of k_{xq} and has to be treated in the same manner (see below).

It is now possible to use the rate constants estimated from static and dynamic fluorescence decays to evaluate the quantum yield pattern of the product as shown in Figure 1. A reasonably good agreement with experimental values may be regarded[19] as a successful proof of the reaction mechanism as proposed. For this purpose it is necessary to estimate the rate constant of the product formation from the exciplex, k_{xa}, that is carried out by using only the points at $[AABF_2] < 0.02$ M, this linear portion is extrapolated to the y-axis to give interecept = 7.7 ± 2.5, the reciprocal of which is the limiting quantum yield 0.13. Since this involves quenching at the infinitive $AABF_2$ concentrations, every excitation is converted to the exciplex and the simple relation of $k_{xa} = \Phi(\sum k_{x1} + k_{xa})$ gives the rate constant of 7.4×10^6 s^{-1}, the accuracy of which is undoubtedly limited owing to scatter of the points in the linear portion and to the distant extrapolation. When this and kinetic data (Table 3) are used to compute the quantum yield by eq 10 under the experimental conditions in dioxane (Figure 1), the resulting plot of $1/\Phi$ *vs* $1/[AABF_2]$ agrees in the low concentration range but deviates from the experimental points considerably as indicated by a solid line. Obviously, in the present case, the quantum yield determination is critically complicated in two respects. First, owing to the close overlap of the absorption bands of PN and $AABF_2$ in the 310–350-nm area the increase of $[AABF_2]$ also competitively absorbs the light energy of RPR 3500-Å lamps without generating the exciplex and, therefore, product. The overall effect is to artificially retard Φ with increasing $[AABF_2]$ by an internal screen effect; indeed, at $[AABF_2] > 0.01$ M, the edge of its absorption spectra starts to advance into the region above 320 nm. Second, the difficulty is compounded by the mechanistic complexity arising from the self-quenching of the exciplex by $AABF_2$ that builds in a secondary dependency on $AABF_2$ concentrations in eq 1 owing to the fact that $\beta = k_{xa}/(\sum k_{x1} + k_{xa} + k_{xq}[A])$; this is derived from eq 10 (see Experimental Section) on the basis of Scheme 1. That is, for a self-quenching case such as the present one, the usual linear correlation of $1/\Phi$ *vs* $1/[AABF_2]$, common to most photoreactions,[13] does not hold since β will be reduced by the term of $k_{xq}[A]$ and must turn upward at higher concentrations; indeed, the calculated plot in Figure 1 shows this effect in the $[AABF_2] > 0.03$ M range. It is therefore clear that theoretically eq 1 cannot afford a straight line and the extrapolation used to obtain $K^{y}_{sv} = 460$ M^{-1} is valid only for a low concentration range. However as shown in Figure 1, the deviation is not trivial even at the range of $[AABF_2] < 0.02$ M where the complications from the self-quenching have not reached a significant stage; this drastic deviation obviously arises from the internal screening effect.

Experimental Section

The same experimental conditions and apparatus as those reported previously[11,20] were used here. Phenanthrene was specially purified to remove anthracene by the reported method.[5a]

Photocycloaddition of Phenanthrene to $AABF_2$. A solution of PN (191 mg, 1.1 mmol) and $AABF_2$ (302 mg, 2.0 mmol) in anhydrous ether (50 mL) was placed into eight quartz tubes and purged with nitrogen. The solution was irradiated in a Rayonet reactor equipped with 300-nm lamps (RPR 3000) for 11 h. GC analysis (at 230 °C, 25 m × 0.2 mm HP-1 capillary column) of the colorless photolysate showed that 12% of PN (t_R 2.59 min)

remained and one major product at t_R 5.14 min (**2**, 81%) was formed along with a minor product at t_R 4.53 min (**3**, 2%). Ether was evaporated, and the residue was flash chromatographed using 15% and 17% AcOEt in hexanes as eluants to give two fractions. The first one afforded 141 mg (46%) of crude *cis*-9-acetyl-9,10-dihydro-10-(2-oxopropyl)phenanthrene (**2**), which was recrystallized from EtOAc/hexanes to give colorless crystals, mp 119–120 °C. Anal. Calcd for $C_{19}H_{18}O_2$: C, 81.98; H, 6.52. Found: C, 81.77; H, 6.45. The second fraction contained 17 mg (5.6%) of *trans*-9-acetyl-9,10-dihydro-10-(2-oxopropyl)-phenanthrene (**3**). A mixture (40 mg) of **2** and **3** was also obtained in a 1:2 ratio.

Compound **2** showed the following physical data: MS, EI 278 (M^+, 3), 220 ($M^+ - CH_3COCH_3$, 26), 217 (25), 178 (PN^+, 100), 165 (14), 43 (54); CI 279 ($M^+ + 1$, 100), 221 ($M^+ + 1 - CH_3COCH_3$, 52); IR (KBr) 3026, 1708 (vs), 1567 (s), 1485 (s), 1400 (s), 1371 (s), 1354 (s), 1161 cm^{-1}; ^1H NMR ($CDCl_3$) δ 1.94 (s, 3H), 2.20 (s, 3H), 2.86 (dd, broad, 1H, J = 18.0 and 5.8 Hz), 3.02 (dd, 1H, J = 18.0 and 6.8 Hz), 3.85 (m, 1H, J = 4.6, 5.8 and 6.8 Hz), 3.99 (d, 1H, J = 4.6 Hz), 7.15–7.44 (m, 6H), 7.55 (dd, 1H, J = 7.5 and 1.1 Hz), 7.81 (d, 1H, J = 7.4 Hz); (C_6D_6) δ 1.68 (s, 3H), 1.70 (s, 3H), 2.41 (dd, 1H, J = 18.0 and 5.8 Hz, 2.91 (dd, 1H, J = 18.0 and 6.8 Hz), 3.85–3.92 (m, 2H), 7.09–7.24 (m, 6H), 7.61 (d, 1H, J = 7.4 Hz), 7.66 (d, 1H, J = 7.5 Hz); ^{13}C NMR ($CDCl_3$) δ 208.79, 207.04, 137.80, 134.34, 134.20, 133.76, 128.59, 128.24, 128.18, 217.94, 127.41, 125.82, 124.43, 124.21, 55.29, 43.49, 35.44, 30.52, 30.33 ppm.

Compound **3** had the following physical data: MS, EI 278 (M^+, 7), 220 ($M^+ - CH_3COCH_3$, 53), 217 (46), 205 (19), 178 (PN^+, 50), 165 (13), 43 (100); CI 279 ($M^+ + 1$, 12), 221 ($M^+ + 1 - CH_3COCH_3$, 100); IR (neat) 3067 (m), 2923 (m), 1713 (vs), 1485 (s), 1450 (s), 1440 (s), 1356 (s), 1160 (s), 760 (s), 738 (s) cm^{-1}; ^1H NMR ($CDCl_3$) δ 1.97 (s, 3H), 2.00 (s, 3H), 2.51 (dd, 1H, J = 17.0 and 6.0 Hz), 2.55 (dd, 1H, J = 17.8 and 8.8 Hz), 3.70 (d, 1H, J = 1.3 Hz), 4.00 (m, 1H, J = 1.3 and 6.0 and 8.8 Hz), 7.23–7.34 (m, 5H), 7.39 (t, 1H, J = 6.2 Hz), 7.73 (d, 1H, J = 7.5 Hz), 7.79 (d, 1H, J = 7.8 Hz); (C_6D_6) δ 1.42 (s, 3H), 1.68 (s, 3H), 2.09 (dd, 1H, J = 17.8 and 6.0 Hz), 2.16 (dd, 1H, J = 17.8 and 8.5 Hz), 4.23 (m, 1H, J = 1.7 Hz, 6.0 and 8.5 Hz), 6.96 (dd, 1H, J = 7.8 and 1.2 Hz), 7.07–7.27 (m, 5H), 7.58 (dd, 1H, J = 7.0 and 1.7 Hz), 7.63 (dd, 1H, J = 7.8 and 0.8 Hz); ^{13}C NMR δ 206.90, 206.68, 137.73, 133.83, 132.55, 132.28, 130.91, 128.91, 128.53, 128.42, 128.13, 127.76, 124.18, 123.94, 57.33, 37.49, 36.13, 30.50, 28.45 ppm.

This experiment was repeated using the same concentrations of PN and $AABF_2$ and $C_{16}H_{34}$ (1.0×10^{-2} M) as the internal standard in 55 mL of ether (nine quartz tubes, nitrogen purged). The solution was irradiated for 6.5 h with 350-nm lamps (RPR 3500). GC analysis under the same conditions at various intervals gave the percentage of PN, **2**, and **3** as follows: at 0.5 h, 53, 5, 0; at 1 h, 47, 8, 0; at 2 h, 37, 17, 1; at 4 h, 21, 32, 2; at 6 h, 10, 40, 2. Workup as above gave a mixture (258 mg, yield 72%) of **2** and **3** in a 1.0:1.3 ratio.

Acid and Base Treatment of Diketones 2 and 3. To a stirred solution of a mixture of **2** (62%) and **3** (30%) (82 mg, 0.29 mmol) in methanol (40 mL) was added sodium methoxide (2 N × 10 mL) solution. After 1.5 h at the room temperature, 40 mL water was added, and the resulting solution was extracted with CH_2Cl_2 (3 × 20 mL). The combined CH_2Cl_2 extract was washed with saturated sodium chloride solution and dried with $MgSO_4$. GC analysis of the crude product showed **3** (t_R 4.53 min, 34%), **2** (t_R 5.14 min, 1%), and 4a,12b-dihydro-3-methylphenanthro-[9,10-*b*]-1-cyclohexen-2-one (**4**, t_R 6.46 min, 60%) as well as a minor new peak at t_R 6.96 min (5%). Flash chromatography of the residue with 15% ethyl acetate in hexanes as the eluant provided **4** (29 mg, yield 38%): MS, EI 260 (M^+, 4), 178 (PN^+, 100), 152 (6); CI 261 ($M^+ + 1$, 100), 178 (PN^+, 13): IR ($CHCl_3$) 3084 (m), 2998 (m), 2940 (m), 1664 (vs, C=CC=O), 1495 (s), 1461 (s), 1450 (s), 1388 (s), 1134 (s), 770 (vs), 751 (vs) cm^{-1}; ^1H NMR ($CDCl_3$) δ 1.89 (broadens, 3H), 2.25 (s, broad, 2H), 3.49 (dt, 1H, J = 7.5 and 5 Hz), 3.79 (d, 1H, J = 5.1 Hz), 6.04 (bs, 1H, J = 0.5 Hz), 7.10 (d, 1H, J = 7.7 Hz), 7.24–7.33 (m, 3H), 7.36–7.40 (m, 2H), 7.81 (d, 1H, J = 8.0 Hz), 7.82 (dd, 1H, J = 8.0 and 1.0 Hz); (C_6D_6) δ 1.17 (s, 3H), 1.59 (dd, broad, 1H, J = 18.2 and 5.2 Hz), 1.90 (dd, broad, 1H, J = 18.2 and 11.0 Hz), 2.96 (dt, 1H, J = 11.0 and 5.0 Hz), 3.80 (d, broad, 1H, J = 5.0 Hz), 6.05 (s, broad, 1H), 6.89 (dd, 1H, J = 7.4 and 1.5 Hz), 7.09–7.17 (m, 5H), 7.65 (dd, 1H, J = 7.8 and 1.2 Hz), 7.67 (dd, 1H, J = 7.8 and 1.2 Hz): ^{13}C NMR δ 199.44, 162.80, 137.53, 134.08, 133.25, 130.48, 129.79, 128.33, 128.11, 128.02, 127.40, 127.26, 126.26, 124.35, 123.70, 49.37, 37.95, 34.74, 24.18 ppm. For the ^1H NMR spectrum in $CDCl_3$, when the signal at 2.25 ppm was irradiated, the CH_3 signal sharpened to a doublet (J = 1.0 Hz) and two methine protons became a AB quartet (J = 5.1 Hz). When the signal 3.79 ppm was irradiated, the signal at 3.48 ppm became a broadened triplet (J = 7.5 Hz).

A sample of **2**–**4** and PN in methanol containing 0.2 N H_2SO_4 was kept at room temperature for 10 h. The GC analysis before the treatment showed the ratio of 0.89:0.152:0.00:1.00 which changed to 0.33:0.155:0.24:1.00; PN was used as the internal standard.

A sample of **3** and $C_{16}H_{34}$ (internal standard) in CH_3OH was treated with $NaOCH_3$ (0.2 N) or H_2SO_4 (0.2 N) at room temperature overnight; no new GC peak appeared in addition to the internal standard. When this solution was heated on a water bath, many peaks and that corresponding to **4** started to show in the GC analysis.

A solution of **2** (0.01 M) in ether either in the absence or presence of PN (0.02 M) was photolyzed with the same apparatus for 5 h. GC analysis of the photolysate showed no change of the percentage of **2**.

Fluorescence Decay Kinetics. Fluorescence decay rates in argon-purged dioxane solutions were measured on a Photon Technology International (PTI)LS-1 fluorimeter by a time-correlated single photon counting method. For deconvolution of the decay profiles, an iterative weighted nonlinear least-squares reconvolution software package (obtained from PTI; version 2.03) was used. The gated flash lamp used in this study contained hydrogen gas, and the lamp profile typically had a FWHM of 1.7–1.8 ns. Steady-state fluorescence quenching experiments were performed on either a Perkin-Elmer MPF-44B (uncorrected) or a PTI LS-100 (corrected) fluorimeter. Samples for fluorescence decay or steady-state fluorescence quenching experiments were prepared individually in 5-mL volumetric flasks with [PN] = $2–5 \times 10^{-5}$ M just before measurements. A 3-mL aliquot of the prepared solution was transferred to a fluorimeter cell and either used directly or purged with argon.

According to Scheme 1, the time dependence of *PN and the exciplex concentrations (that are proportional to fluorescence intensities) could be described by the coupled differential equations (5a) and (5b). In the case of δ-pulse excitation, solution

$$d[*PN]/dt = I(t) + k_{xr}[*PN - A] - (\sum k_{p1} + k_{pq}[A])[*PN] \quad (5a)$$

$$d[*PN - A]/dt = k_{pq}[A][*PN] - (\sum k_{x1} + k_{xa} + k_{xr} + k_{xq}[A])[*PN - A] \quad (5b)$$

of the differential equations gave (6a) and (6b)

$$[*PN](t) = C_1 e^{-\lambda_1 t} + C_2 e^{-\lambda_2 t} \quad (6a)$$

$$[*PN - A](t) = C_3(e^{-\lambda_1 t} - e^{-\lambda_2 t}) \quad (6b)$$

where

$$2\lambda_{1,2} = \sum k_{p1} + (k_{pq} + k_{xq})[A] \pm [(\sum k_{p1} + (k_{pq} - k_{xq})[A] - \sum k_{x1} - k_{xr} - k_{xa})^2 + 4k_{pq}k_{xr}[A]]^{1/2} \quad (7)$$

In the absence of $AABF_2$, natural decay lifetime λ_1^{-1} was monitored at 370 nm by 300-nm excitation. In the presence of $AABF_2$, PN was excited at 350 nm in order to avoid $AABF_2$ absorption; this excitation generates a Raman band to obscure the 370-nm region (PN emission). Therefore, the decay curve of the exciplex monitored at 470 nm was fitted to a biexponential pattern comprising $\tau_1 = \lambda_1^{-1}$ corresponding to residual *PN emission lifetime and a longer lived component $\tau_2 = \lambda_2^{-1}$ corresponding to decay lifetimes of the exciplex. The observed lifetimes at various [$AABF_2$] are listed in Table 2.

From eq 4, the following relationship between the observed rates and parameters in Scheme 1 could be obtained.

$$\lambda_1 + \lambda_2 = (\sum k_{p1} + \sum k_{x1} + k_{xr} + k_{xa}) + (k_{pq} + k_{xq})[A] \quad (8)$$

$$\lambda_1\lambda_2 = \sum k_{p1}(\sum k_{x1} + k_{xr} + k_{xa}) + (k_{xq}\sum k_{p1} + k_{pq}\sum k_{x1})[A] + k_{pq}k_{xq}[A]^2 \quad (9)$$

The plots according to eqs 7–9 are shown in Figures 5–7 from which the rate constants in Scheme 1 were obtained.

The plots of $\lambda_1 + \lambda_2$ vs [$AABF_2$] and $\lambda_1\lambda_2$ vs [$AABF_2$] are shown in Figures 6 and 7. The latter plot (Figure 7) could be fitted to a quadratic equation in which the coefficients could be obtained; the error margins were compounded and gave less accurate calculated rate constants. The plot of Figure 6 gave an intercept = $\sum k_{p1} + \sum k_{x1} + k_{xr} = (7.46 \pm 0.79) \times 10^7\ s^{-1}$ and a slope = $k_{pq} + k_{xq} = (5.57 \pm 0.22) \times 10^9\ m^{-1}\ s^{-1}$. From these figures and those shown in Table 3, the calculations gave $k_{xr} < 10^6\ s^{-1}$ and $k_{xq} \cong 6.2 \times 10^7$ or about $10^8\ s^{-1}$, both of which were within the error margins and were only approximations.

Solvent Effects on Exciplex Fluorescence. The solutions in [PN] = 4.0×10^{-4} M and [$AABF_2$] = 0.042 M in carbon tetrachloride, dioxane, chloroform, and methylene chloride were made. Their fluorescence spectra were taken, and their exciplex peak wavenumbers (ν_{max}) were plotted against those of the $DBMBF_2$–*p*-xylene systems[16] (Figure 4) serving as reference which has μ(dipole moment) = 10.5 D. The slope was equal to μ^2(PN–$AABF_2$)/μ^2 (ref) = 1.14 on the basis of equal solvent cavities for the two systems: μ(PN–$AABF_2$) was calculated to be 11.2 D.

Determination of Quantum Yields of 2. A stock solution of PN (0.02 M) and hexadecane (internal standard, 0.01 M) in dioxane was prepared. This solution was used to dissolve $AABF_2$ to make 0.04 M solution. Appropriate amounts of the second solution were diluted with the first one to give samples containing PN (0.02 M), hexadecane (0.01 M), and various concentrations of $AABF_2$ (0.0064–0.04 M). The samples (5 mL) were placed in 10 Pyrex tubes and purged with nitrogen. These tubes were irradiated with a RPR 3500 light source for 14 min to cause less than 8% reaction of PN as determined by GC analysis. The yield of **2** as determined by GC was used to calculate the quantum efficiency against an actinometry[13b] of benzophenone (0.05 M) and benzhydrol (0.10 M). The plot of $1/\Phi$ against 1/[$AABF_2$] was shown in Figure 1.

On the basis of Scheme 1, the quantum efficiency of **2** could be calculated by eq 10, assuming k_{xr} was negligible. The rate of

$$\Phi = \frac{k_{xa}k_{pq}[A]}{(\sum k_{p1} + k_{pq}[A])(\sum k_{x1} + k_{xa} + k_{xq}[A])} \quad (10)$$

the formation **2** from the exciplex is estimated as follows: the first six points in dioxane ([$AABF_2$] < 0.02 M) are extrapolated to the *y*-axis to given $1/\beta = 7.7 \pm 25$; $\beta = 0.13$ is the limiting quantum yield, and $k_{xa} = \sum k_{x1}\beta = 5.7 \times 10^7 \times 0.13 = 7.4 \times 10^6\ s^{-1}$. Using the rate constants given in Table 3, theoretical Φ values could be calculated and used to make the plot of solid line in Figure 1.

Fluorescence Quenching. Dioxane solutions containing PN (5.4×10^{-4} M) and $AABF_2$ (0.0005, 0.001, 0.002, 0.006, 0.012 M) were purged with argon to take fluorescence spectra with excitation at 350 nm (for PN) and 310 nm (for $AABF_2$ and PN) in a Perkin-Elmer MPF44B at right angle configuration; Figure 2 is a specimen for the former case. For a solution of [$AABF_2$] < 0.002 M, the OD at 310 nm was lower than 0.85; $AABF_2$ did not show absorptions above 335 nm up to 0.2 M. Similar experiments were carried out with a solution containing [PN] = 5.4×10^{-3} M and front-face illumination (45° configuration); the excitation at 335 and 350 nm gave spectra similar to that shown in Figure 2.

Flash Photolysis. Dioxane and acetonitrile solutions containing PN($\sim 10^{-2}$ M) and $AABF_2$($\sim 10^{-2}$ M) were excited with YAG laser (Spectro Physics, GCR-12) at 355 nm < 20 mJ/pulse. This new system was recently completed by Dr. C. Bohne in the Chemistry Department, University of Victoria, and has been described in the Inter-Americal Photochemical Society Newsletter (Vol. 16, No. 1, May 1993). A detailed description will be published soon.

Acknowledgment. The authors are much indebted to Natural Science and Engineering Council of Canada for generous financial support. Time-resolved fluorimetry and flash photolysis were performed on machine time made available through the courtesy of Drs. P. Wan and Cornelia Bohne of the University of Victoria; we are most grateful for their cooperation and assitance.

Supplementary Material Available: Fluorescence spectra and flash photolysis results (5 pages). This material is contained in libraries on microfiche, immediately follows this article in the microfilm version of the journal, and can be ordered from the ACS; see any current masthead page for ordering information.